

State-variable friction for the Burridge-Knopoff model

Ian Clancy* and David Corcoran†

Department of Physics, University of Limerick, Ireland

(Received 11 December 2008; revised manuscript received 19 April 2009; published 20 July 2009)

This work shows the relationship of the state variable rock-friction law proposed by Dieterich to the Carlson and Langer friction law commonly used in the Burridge-Knopoff (BK) model of earthquakes. Further to this, the Dieterich law is modified to allow slip rates of zero magnitude yielding a three parameter friction law that is included in the BK system. Dynamic phases of small scale and large scale events are found with a transition surface in the parameter space. Near this transition surface the event size distribution follows a power law with an exponent that varies as the transition is approached contrasting with the invariant exponent observed using the Carlson and Langer friction. This variability of the power-law exponent is consistent with the range of exponents measured in real earthquake systems and is more selective than the range observed in the Olami-Feder-Christensen model.

DOI: [10.1103/PhysRevE.80.016113](https://doi.org/10.1103/PhysRevE.80.016113)

PACS number(s): 89.75.Da, 62.20.Hg

I. INTRODUCTION

The slow shearing of two tectonic plates results in earthquakes, which are a manifestation of stick-slip dynamics. The earthquake system is simulated by the Burridge-Knopoff (BK) model [1]. The BK model comprises a spring-block arrangement and an appropriate friction law allowing dissipation of energy in each block. In many studies of the BK model the friction law considered has been a simplified approximation of rock friction without any hysteretic effects [2–7]. Some have included friction laws that include a state variable [8] but either are not based on a realistic friction law or fail to reproduce behavior seen in earthquake systems [9]. In the case of the BK model’s cellular automata variant, the Olami-Feder-Christensen (OFC) model [10], any details of the dynamic friction have been completely ignored,

$$\varphi(V, f) = \begin{cases} \left(1 + \frac{V}{v_f}\right)^{-1} & \text{if } V > 0, \\ 1 & \text{if } V = 0, f \geq 1, \\ f & \text{if } V = 0, f < 1. \end{cases} \quad (1)$$

The Carlson and Langer (CL) friction law [Eq. (1)], here expressed in nondimensional form, is frequently used with the BK model. Here φ is the frictional shear stress, V is the slip rate, v_f is a characteristic slip rate scale, and f is the applied shear force. The CL law is velocity weakening in that the magnitude of the nondimensional frictional force φ decreases with increasing slip rate v . The velocity weakening is a necessary property of the friction for the system to display dynamic instability revealed in the real world as earthquakes. Previously, we have shown that the BK system employing this friction law is a tuned critical system [11], the tuning (or control) parameter being a property of the friction. The necessity of tuning to obtain critical behavior in a homogeneous BK system, however, implies the absence of criticality in general and in particular self-organized criticality [12].

To achieve a more representative system of an earthquake fault, one may include a more realistic state variable friction. Ohmura and Kawamura [9] have looked at the dynamics of the BK model with the Dieterich and Ruina friction law [13–15] but they did not find the expected power-law distribution of earthquake size (moment), instead finding large scale near periodic events dominating. Here we consider the Dieterich law of [16], which is a state variable friction law that can reproduce laboratory rock-friction experimental results well. This work explores the relationship between the CL and Dieterich friction laws, and the dynamics of the BK model in the parameter space of the Dieterich law.

In Sec. II we will show the relationship between the CL law and the steady-state Dieterich law. In Sec. III the Dieterich law will be modified to be defined at zero slip rate while maintaining logarithmic healing of the friction. This represents a development for the BK model system. The dynamics of the single-block and multiblock BK models are then investigated in Secs. IV and V establishing the influence of the feedback introduced by the state variable, and whether the two dynamic phases previously observed in the tuned BK model [17] are observed. The range of b values observed in the BK model are then compared with that seen in nature and in the OFC model.

II. FROM THE DIETERICH FRICTION LAW TO THE CARLSON-LANGER FRICTION LAW

Here we introduce the Dieterich law and show its relationship with the CL law. The Dieterich law is a state variable law and has an associated fading memory of previous states. However, if the slip rate is maintained at a constant velocity V then the state variable approaches its steady state and the resulting function of V is the steady-state Dieterich friction law. Here we modify the Dieterich law for its use in the BK model. Certain limiting boundary conditions are necessary to keep the friction defined at zero slip rate and so that the coefficient of friction approaches zero at large slip rates. The resulting friction law is then compared to the CL law.

The Dieterich friction law is given by Eq. (2),

*ian.clancy@ul.ie

†david.corcoran@ul.ie

$$\mu = \mu_0 - A \ln\left(\frac{V_0}{V} + 1\right) + B \ln\left(\frac{\Theta}{b} + 1\right), \quad (2a)$$

$$\frac{d\Theta}{dt} = 1 - \frac{V\Theta}{D_c}, \quad (2b)$$

where μ is the coefficient of friction, V is the slip rate, and Θ is the state variable dependent on time t . The parameters μ_0 , A , B , V_0 , b , and D_c are all constants. If one considers Eq. (2) in the steady state, then $\Theta = \Theta_{ss}$ and $\frac{d\Theta}{dt} = 0$; hence $\Theta_{ss} = D_c/V$ yielding μ_{ss} in Eq. (3). Letting $V_1 = D_c/b$ and $C = B - A$:

$$\mu_{ss} = \mu_0 + A \ln\left(\frac{V_1 + V}{V_0 + V}\right) + C \ln\left(\frac{V_1}{V} + 1\right). \quad (3)$$

We now impose two conditions on the steady-state friction that reflects first the velocity weakening necessary for unstable stick-slip motion and second the concept of a coefficient of static friction,

$$\lim_{V \rightarrow \infty} \mu_{ss} = 0, \quad (4a)$$

$$\lim_{V \rightarrow 0} \mu_{ss} = \text{constant}. \quad (4b)$$

The former condition, given by Eq. (4a), necessitates $\mu_0 = 0$. Rock-friction experiments have found μ_0 to vary over a wide range depending on the material and environmental conditions, for example, μ_0 for granite may vary in the range of approximately [0.3, 0.7] (see [18]). Nevertheless, as the study here is concerned with the dynamics of the BK model, and the choice of $\mu_0 = 0$ does not affect the *dynamics* of the system in any way [19], the choice of μ_0 is arbitrary [4].

Imposing Eq. (4b) requires $C = 0$ (or equivalently $A = B$). Experimentally, although it is found that B is usually greater than A , A and B are of the same order of magnitude and so in the first instance the assumption that $A \approx B$ is valid. Moreover, it is usually suggested that B must be greater than A to allow the instability of stick-slip motion to occur but this criterion for instability is based on an approximation of Eq. (2). Employing a linear stability analysis (as in [15]) to Eq. (2) without approximation, the instability criterion for infinitely slow driving is $BV_1 > AV_0$, or if $A = B$, then $V_1 > V_0$ as is the case here. As will be seen, this assumption allows the steady-state coefficient of friction to remain finite at an infinitely slow driving rate and, with modification, the state variable friction also remains finite.

Taking note of this limiting behavior, the maximum frictional shear stress is $\varsigma\mu$, where ς is the normal stress at the fault,

$$\varsigma\mu_{ss} = \varsigma A \ln\left(\frac{V_1 + V}{V_0 + V}\right).$$

Naturally, at zero slip speed, $\varsigma\mu_{ss}(0) = \varsigma A \ln\left(\frac{V_1}{V_0}\right)$, this value may be used to define a normalized functional form for Eq. (3) such that the function has values in the range [0, 1], as with the CL friction law, yielding

$$\phi_{ss}^D(V) = \frac{\varsigma\mu_{ss}}{\varsigma A \ln\left(\frac{V_1}{V_0}\right)} = \frac{\ln\left(\frac{V_1 + V}{V_0 + V}\right)}{\ln\left(\frac{V_1}{V_0}\right)} \Rightarrow \phi_{ss}^D(v) = \frac{\ln\left(\frac{\gamma + v}{1 + v}\right)}{\ln(\gamma)}, \quad (5)$$

where $\gamma = \frac{V_1}{V_0}$ and $v = \frac{V}{V_0}$ is the nondimensional velocity. It was determined previously [11] for the nondimensional BK model that the tuning parameter is $v_f = -\left[\frac{d\phi(v)}{dv}\right]_{v=0}^{-1}$, where $\phi(v)$ is the dynamical case of the CL friction defined by Eq. (1). The equivalent measure may be obtained for Eq. (5) yielding

$$v_f = -\left[\frac{d\phi_{ss}^D(v)}{dv} \frac{dv}{dV}\right]_{v=0}^{-1} = V_0 \frac{\gamma \ln \gamma}{\gamma - 1}.$$

The Dieterich friction law is firmly based on experimental observation of rock-friction experiments while the CL friction law [Eq. (1)] is not, merely being a representation of the velocity weakening aspect of friction. Nevertheless, the two friction laws are intimately related. The function ϕ_{ss}^D may be obtained in the limit $\gamma \rightarrow 1$

$$\lim_{\gamma \rightarrow 1} \phi_{ss}^D = \lim_{\gamma \rightarrow 1} \left[(\ln \gamma)^{-1} \ln \frac{\gamma + v}{1 + v} \right] = (1 + v)^{-1} = \left(1 + \frac{V}{v_f}\right)^{-1}. \quad (6)$$

Physically, the limit $\gamma \rightarrow 1$ means that the friction law has only one velocity scale rather than the more general two velocity scales. This single scale is related to the dimensional velocity scale D_c/b , being the ratio of the critical slip length scale (see [20]) to the memory time scale. Clearly, in the limit $\gamma \rightarrow 1$ comparison of Eq. (6) with Eq. (1) shows the steady-state Dieterich friction law *becoming* the CL friction law. Indeed, there is a finite maximum difference between the friction laws $\phi_{ss}^D(v)$ and $\phi(v)$, and this maximum is at an intermediate velocity whereas at small and high velocities the two laws become the same.

From the preceding analysis we draw the conclusion that the CL friction law frequently used in the BK model can be a good approximation of the more realistic law of Eq. (5), yet realistic time dependent state effects are not incorporated into either of these friction laws. Section III seeks to include such phenomena.

III. VARIANT OF THE DIETERICH LAW

The BK model has been studied previously using the CL friction law [11, 17]; however, as pointed out above this is not a generally realistic friction law and is a limiting case of the more realistic Dieterich law. Here we show how a variant of the Dieterich law can be incorporated explicitly into the BK model.

The Dieterich friction law [Eq. (2)] includes a state variable Θ that is, in effect, an evolving time scale as indicated by its dimensions. This dynamic time scale represents the delayed reaction of the friction to instantaneous changes in velocity. The “state” of the friction is merely a dynamically

evolving scale that in turn may influence the systems dynamics.

It is known that driving a BK system at a finite rate can change its dynamics, bringing the system through a dynamic transition as the driving rate is increased [21–23]. It has been claimed by Vasconcelos [24] that identification of the transition point [25] can be inaccurate if using a relatively fast finite driving rate. Here and in our previous work [11,17], infinitely slow driving is implemented to avoid the added complications of dynamic transitions due to finite driving rates.

For the infinitely slowly driven BK model it is preferable to use velocity scales rather than time scales for the state variable of the Dieterich friction law. To do so one defines a velocity scale containing a fixed length scale and the dynamic time scale leading to an evolving velocity scale. Such a procedure requires a change in variable from Θ to a velocity state variable ϑ . Letting $\vartheta = \frac{V\Theta}{b}$ and noting that the time derivative of ϑ is given by

$$\frac{d\vartheta}{dt} = \frac{V}{b} \frac{d\Theta}{dt} + \frac{\vartheta}{V} \frac{dV}{dt}$$

allows the Dieterich friction law to be recast in the form of Eq. (7), again imposing on the steady-state coefficient of friction, μ_{ss} , with the conditions given by Eqs. (4a) and (4b),

$$\mu = A \ln\left(\frac{\vartheta + V}{V_0 + V}\right), \quad (7a)$$

$$\frac{d\vartheta}{dt} = \frac{V}{b} \left[1 - \frac{\vartheta}{V_1}\right] + \frac{\vartheta}{V} \frac{dV}{dt}. \quad (7b)$$

The maximum frictional shear stress, defined by the Dieterich law, is given by $\Phi^D(V, \mathcal{T}) = \varsigma \mu$, where ς is the normal stress and \mathcal{T} is the applied shear stress, yielding Eq. (8),

$$\Phi^D(V, \mathcal{T}) = \begin{cases} \varsigma A \ln\left(\frac{\vartheta + V}{V_0 + V}\right) & \text{if } V > 0 \text{ or} \\ \left[V = 0 \text{ and } \mathcal{T} > \varsigma A \ln\left(\frac{\vartheta}{V_0}\right) \right] & \\ \mathcal{T} & \text{otherwise,} \end{cases} \quad (8a)$$

$$\frac{\partial \vartheta}{\partial t} = \frac{V}{b} \left[1 - \frac{\vartheta}{V_1}\right] + \frac{\vartheta}{V} \frac{dV}{dt}. \quad (8b)$$

The BK equations of motion for the k th block (denoted by a subscript) can be written in terms of the friction law of Eq. (8), and following the approach in [17], results in Eqs. (9) and (10), which are written in dimensional form,

$$\Phi^D(V_k, \mathcal{T}_k = \rho \Delta y F_k) = \begin{cases} \varsigma A \ln\left(\frac{\vartheta_k + V_k}{V_0 + V_k}\right) & \text{if } V_k > 0 \text{ or} \\ \left[V_k = 0 \text{ and } \mathcal{T}_k > \varsigma A \ln\left(\frac{\vartheta_k}{V_0}\right) \right] & \\ \mathcal{T}_k & \text{otherwise,} \end{cases} \quad (9)$$

$$\frac{dV_k}{dt} = F_k - \frac{\Phi^D(V_k, \rho \Delta y F_k)}{\rho \Delta y}, \quad (10a)$$

$$\frac{dF_k}{dt} = \frac{\lambda + 2\mu}{\rho \Delta x^2} (V_{k+1} + V_{k-1} - 2V_k) + \frac{2\mu}{\rho \Delta y^2} (\bar{v} - V_k), \quad (10b)$$

$$\frac{d\vartheta_k}{dt} = \frac{V_k}{b} \left[1 - \frac{\vartheta_k}{V_1}\right] + \frac{\vartheta_k}{V_k} \frac{dV_k}{dt}, \quad (10c)$$

where ρ is the mass density, Δy is the width of the shear zone near the fault, Δx is the discretization along the fault, \bar{v} is the relative velocity of the two tectonic plate surfaces in contact, and λ and μ are the Lamé parameters.

To modify the Dieterich law a nondimensionalization of Eqs. (9) and (10) is first performed using Eq. (A1) (see Appendix A), resulting in Eqs. (11), (12), and (15). An important point to note in the nondimensionalization is the separation of time scales of the two main stages of motion for a body under the influence of the friction: active slip (nonzero slip rate) and quiescence (zero slip rate). In these equations v_k is the nondimensional velocity, f_k is the nondimensional applied force, T_k is the nondimensional applied shear stress, ϕ^D is the nondimensional shear stress associated with the Dieterich friction law, θ_k is the state variable of the friction law, s and γ are nondimensional frictional parameters defined by Eqs. (A1k) and (A1h), respectively, the subscript k refers to the k th block, k_c and k_t are numerical discretizations, and t_A and t_Q are the nondimensional time as measured in the active and quiescent periods, respectively.

Initially quiescence will be considered where $t = \tau_Q t_Q$ thus

$$\phi^D(v_k, T_k = k_t^{-1/2} f_k) = \begin{cases} & \text{if } v_k > 0 \text{ or} \\ \frac{s}{\ln \gamma} \ln\left(\frac{\theta_k + v_k}{1 + v_k}\right) & v_k = 0, \text{ and} \\ & T_k > \frac{s}{\ln \gamma} \ln \theta_k \\ T_k & \text{otherwise,} \end{cases} \quad (11)$$

$$\frac{\tau_A}{\tau_Q} \frac{dv_k}{dt_Q} = f_k - k_t^{1/2} \phi^D(v_k, k_t^{-1/2} f_k), \quad (12a)$$

$$\frac{df_k}{dt_Q} = \frac{\tau_Q}{\tau_A} [k_c (v_{k+1} + v_{k-1} - 2v_k) - k_t v_k] + k_t, \quad (12b)$$

$$\frac{d\theta_k}{dt_Q} = \frac{\tau_Q}{\tau_A} v_k \left(1 - \frac{\theta_k}{\gamma}\right) + \frac{\theta_k}{v_k} \frac{dv_k}{dt_Q}. \quad (12c)$$

But, during quiescence, $v_k = 0 \forall k$ and the applied stress, T_k , is balanced by the shear friction stress, ϕ^D , until the threshold defined by Eq. (11) is attained, and so

$$\frac{dv_k}{dt_Q} = 0, \quad (13a)$$

$$\frac{df_k}{dt_Q} = k_t, \quad (13b)$$

$$\frac{d\theta_k}{dt_Q} = \frac{\theta_k}{v_k} \frac{dv_k}{dt_Q}. \quad (13c)$$

The right-hand side of Eq. (13c) is undefined during quiescence as both $v_k=0$ and $\frac{dv_k}{dt_Q}=0$. Nevertheless, it is an experimental observation for rock friction that static surfaces in contact may deform and become better mated leading to the observed maximum friction increasing logarithmically in time while contact is static [20]. In the context of Eq. (13) this implies that θ_k must increase linearly in time while the k th block is static. In Eq. (13c) the rate of change in θ_k during quiescence must then be constant. To satisfy this, a constant κ is written in place of $\frac{\theta_k}{v_k} \frac{dv_k}{dt_Q}$. This constitutes the major *modification* (as opposed to specialization) of the Dieterich friction law that removes the singularity at $v_k=0$ permitting infinitely slow driving. However, it must be reemphasized that this modification is empirically motivated and not an arbitrary substitution. Equation (13c) now reads

$$\frac{d\theta_k}{dt_Q} = \kappa. \quad (14)$$

Turning the attention to the active period (with $t=\tau_A t_A$), again using nondimensionalizations defined by Eq. (A1), results in

$$\frac{dv_k}{dt_A} = f_k - k_t^{1/2} \phi^D(v_k, T_k = k_t^{-1/2} f_k), \quad (15a)$$

$$\frac{df_k}{dt_A} = k_c(v_{k+1} + v_{k-1} - 2v_k) + k_t \left(\frac{\tau_A}{\tau_Q} - v_k \right), \quad (15b)$$

$$\frac{d\theta_k}{dt_A} = v_k \left[1 - \frac{\theta_k}{\gamma} \right] + \frac{\tau_A}{\tau_Q} \kappa, \quad (15c)$$

noting that $\frac{\theta_k}{v_k} \frac{dv_k}{dt_A} = \frac{\tau_A}{\tau_Q} \frac{\theta_k}{v_k} \frac{dv_k}{dt_Q}$ because $t_A = \frac{\tau_Q}{\tau_A} t_Q$. But if the system is infinitely slowly driven [26] $\frac{\tau_A}{\tau_Q} \rightarrow 0$, and so the equations of motion of a block with nonzero slip rate is given by Eqs. (11) and (16),

$$\frac{dv_k}{dt_A} = f_k - k_t^{1/2} \phi^D(v_k, T_k = k_t^{-1/2} f_k), \quad (16a)$$

$$\frac{df_k}{dt_A} = k_c(v_{k+1} + v_{k-1} - 2v_k) - k_t v_k, \quad (16b)$$

$$\frac{d\theta_k}{dt_A} = v_k \left[1 - \frac{\theta_k}{\gamma} \right]. \quad (16c)$$

At threshold the system has at least one block, i , with

$$f_i = \frac{k_t^{1/2} s}{\ln \gamma} \ln \theta_i.$$

A block satisfying this relationship corresponds to the applied shear stress through the bulk medium due to the driving

being balanced by the maximum shear stress due to the friction at the surface leaving a net shear stress of zero at the surface of the block. However, as the system is infinitely slowly driven a perturbation to the stress (or velocity) is necessary to initiate events. Such a perturbation must be small enough that the overall response of the system is independent of its size. Here, the perturbation is made to the stress of the threshold block. If there are many threshold blocks the perturbation is applied to only one. The perturbation of the stress T_k comprises the following operation

$$T_k \mapsto T_k + \sigma \frac{s \ln \theta_k}{\ln \gamma},$$

where σ controls the size of the perturbation scaled by the local static friction. It is assumed that the perturbation is small and so $\sigma \ll 1$.

To summarize, for infinitely slow driving of the system there exists two sets of differential equations corresponding to the slow behavior of quiescence [Eq. (14)] and the fast behavior of activity [Eq. (16)]. The parameter space has three degrees of freedom: γ , the steady-state attractor for the state variable, s , the maximum steady-state value of the friction law, and κ , the healing rate of the state variable. In the following investigation this parameter space will be examined initially in a single-block system and then in multiblock systems where finite-size effects and spatial interactions may also be examined.

IV. SINGLE-BLOCK SYSTEM

The system defined by Eqs. (14) and (16) is investigated initially for a single-block system with $k_c = k_t = 1$, which also means that the shear stress and force are equal and interchangeable, $T_k = f_k$. There remains three free parameters, unlike the BK system previously examined [11,17], which has just one. Nevertheless, unless the system dynamically brings itself to some preferred state regardless of the parameters, dynamic phases of different size events may be expected as previously reported for the BK model with CL friction law [17,25]. The size of an earthquake event is the moment M representing the net slip along the fault during an earthquake event, here defined by

$$M = \sum_k \int_{t_0}^{t_0 + \delta t_A} v_k dt_A, \quad (17)$$

where the event starts at $t_A = t_0$, has a duration of δt_A and the sum is over all blocks.

The existence of these phases is readily observed in Fig. 1 where the steady-state moment is plotted as a function of $\gamma - 1$ and κ keeping $s = 1.6$. The boundary between these phases marks a phase transition and as the moment contours of Fig. 2 show, this is a sharp transition with the moment dropping three decades over a small region of parameter space. This *may* be indicative of a first-order transition similar to the case for the single-block BK system under the influence of the CL friction law. Transitions between small scale and large scale phases are observed by varying any of the three frictional parameters γ , κ , and s , which form a

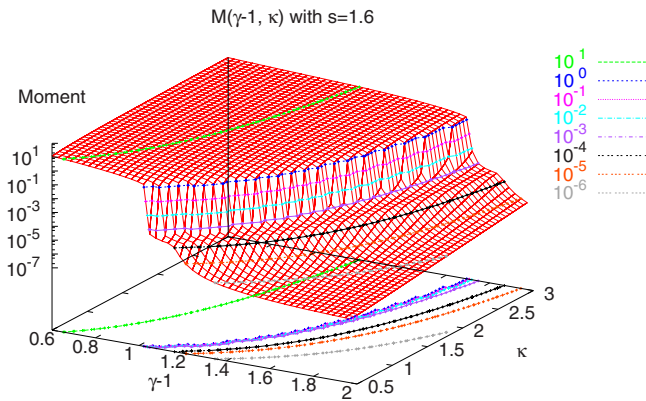


FIG. 1. (Color online) The statistically steady-state event moment, M , of a single-block system as a function of $\gamma-1$ and κ , at fixed $s=1.6$. A perturbation of 10^{-8} to the threshold block stress is applied. Moment contours are indicated at the base of the figure and in Fig. 2.

three-dimensional parameter space for the system with associated coordinates. Figure 3 shows this parameter space for the single-block system partitioned by a transition surface into large scale and small scale event phases. Dots in blue (above the transition surface) are associated with frictional parameters leading to small events ($<10^{-2}$) and dots in red (below the transition surface) are associated with frictional parameters leading to large events ($>10^{-2}$). The transition surface itself was generated by linear interpolation of the event size between adjacent large (red) and small (blue) scale event points in phase space to an event of moment equal to 10^{-2} .

The single-block system goes through an initial transient and its state space trajectory approaches a limit cycle, the details of which are dependent on the system's position in the parameter space (see Fig. 4). In general, it is observed that the limit cycles are confined to more and more restricted region of state space as the transition to the small scale event phase is approached.

For multiblock systems these limit cycles are no longer observed as the system exhibits complexity. However, the

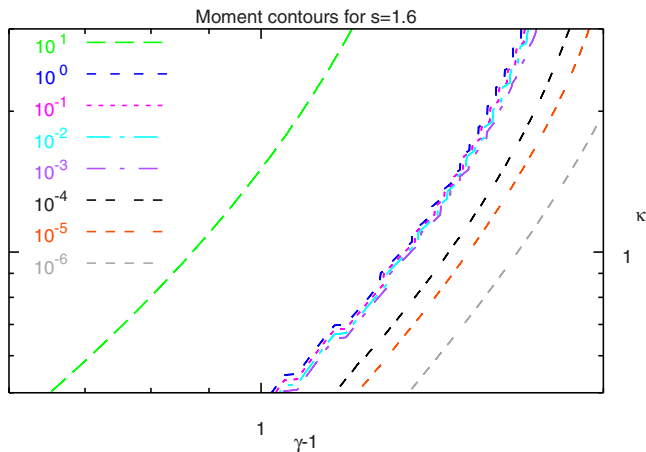


FIG. 2. (Color online) The contours of the moment surface in Fig. 1. The moment contours from 1 to 10^{-3} are nearby in parameter space, indicative of a sharp change in behavior.

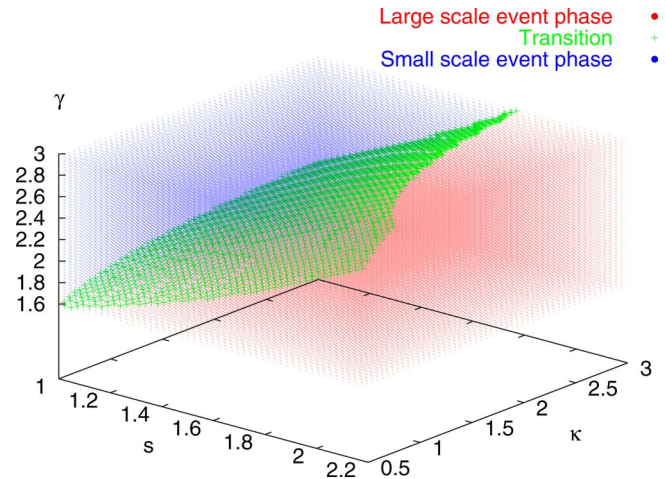


FIG. 3. (Color online) The transition surface with moment 0.01, determined by linear interpolation, separates the parameter space into a large scale event phase (below the surface) and a small scale event phase (above the surface).

single-block system provides clues as to what may be expected of the multiblock system, namely, the existence of two phases and a transition surface/region in parameter space. In view of this, attention is now turned to characterization of the multiblock system. Following the methodology of our previous work [11] this would allow any shifting of the transition, due to the finite size of the system, to be observed.

V. CHARACTERIZING THE MULTIBLOCK SYSTEM TRANSITION

In Sec. IV the single-block system of the BK model was investigated using the newly derived healing friction. It was seen that, by varying the system parameters, a phase transition was observed from large to small events. Figure 5 shows a similar phase transition for the multiblock system. However, the system now demonstrates a power-law region as

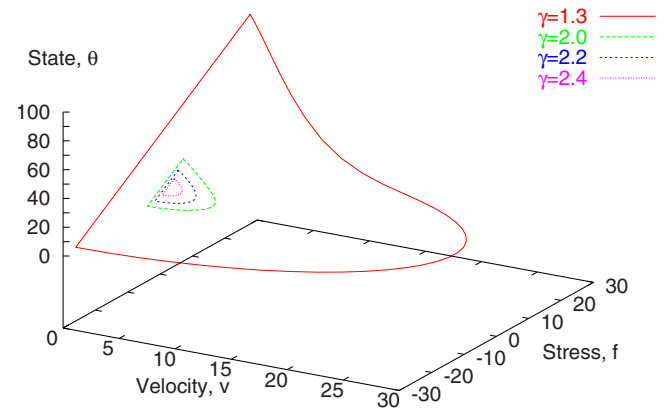


FIG. 4. (Color online) The state space trajectory, which is a stable limit cycle, for the single-block system with $s=1.6$ and $\kappa = 1.75$, varying $\gamma \in \{1.3, 2, 2.2, 2.4, 2.6\}$. As the transition surface is approached, the cycle is contained in a smaller and smaller region of state space.

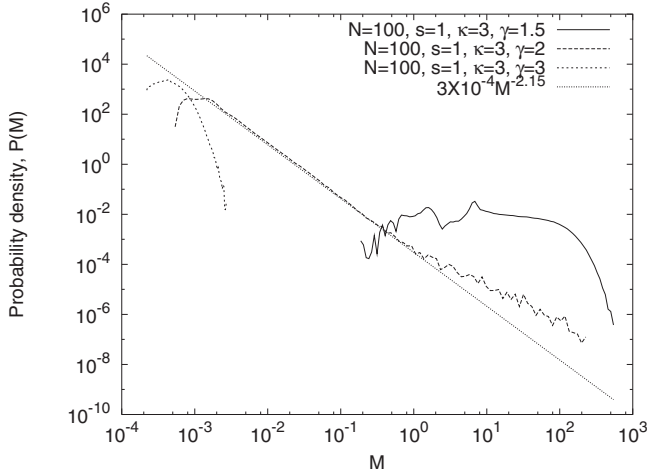


FIG. 5. Results from a 100 block system. Large scale and small scale event moment PDDs are observed with intermediate spanning behavior broadly following a power law. Single block events are not included in the statistical analysis.

previously observed for the BK model with the CL friction law, suggesting a critical transition. What follows is a characterization of this transition.

Here, measures of a 10 and a 100 block system are investigated. There are a number of paths through the transition surface that may be taken and are essentially arbitrary but a path with the transition at $\gamma \approx 2$ is chosen to avoid extreme values of γ in calculations. This path through parameter space is defined by $(s=1, \kappa=3, \gamma)$ with γ varying through the transition. Results from the system with $(s=1, \kappa=3, \gamma \approx 2)$ (see Fig. 6) yield moment probability density distribution (PDD) indicating a transition and are approximately power law in nature with a minor excess of large events.

To characterize the transition an appropriate measure would be the system's mean local stress difference before an event, ψ_Δ , between the local stress, f , and local stress threshold, $F_0 = \frac{s \ln \theta_k}{\ln \gamma}$; hence

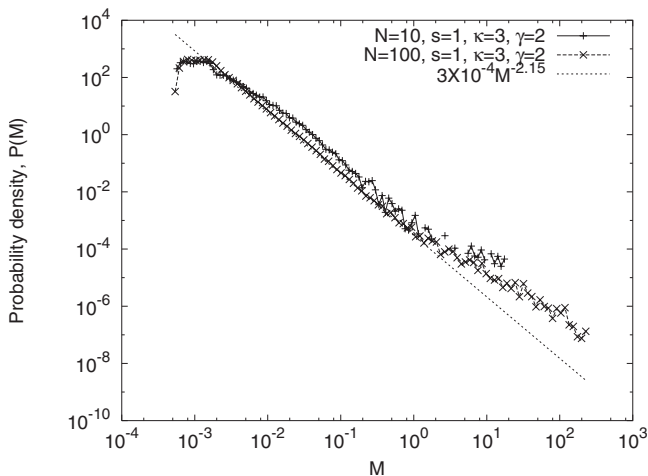


FIG. 6. Moment PDDs for the 10 and 100 block systems with $s=1, \kappa=3$, and $\gamma=2$.

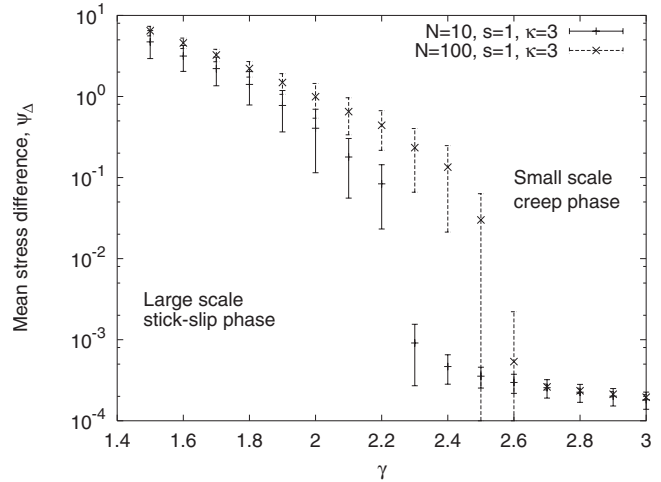


FIG. 7. ψ_Δ as a function of γ through the transition for the 10 and 100 block systems. A transition is clear but not near the estimated transition point of $\gamma=2$.

$$\psi_\Delta = \overline{\langle F_0 - f \rangle},$$

where averages are over space (represented by the bar, $\bar{\cdot}$) at the initiation of each event, averaged over many events, denoted as $\langle \cdot \rangle$.

Figure 7 plots ψ_Δ as a function of γ showing the transition to the small scale moment event phase. In the small scale phase the measure suggests that the system as a whole remains close to the frictional threshold with only small releases of stress that do not remove the system from this position. This is representative of a creeping or stable sliding phase for a finitely driven system. The transition to this phase occurs at higher values of γ than the moment PDDs would suggest, $\gamma=2.3$ for the ten block system and $\gamma=2.6$ for the 100 block system. Nevertheless, this is similar to the behavior seen for the CL friction law BK model where the region of power-law behavior is below the transition indicated by a study of a similar measure in that system (see [11]). In addition to this similarity, it would also appear that the transition point shifts with increasing system size.

Using scales associated with a real earthquake system, Ohmura and Kawamura [9] determined appropriate parameter values for their nondimensionalized friction law. Here it is assumed [27] that the normal stress at the fault perpendicular to the fault plane is $\varsigma=112$ MPa, the shear modulus $\mu=26$ GPa, and the mass density of the rock is $\rho=2700$ kg m⁻³ leading to an S -wave speed of $\sqrt{\frac{\mu}{\rho}}=3.1 \times 10^3$ m s⁻¹. Using estimates by Ohmura and Kawamura [9] for characteristic slip length and time, we estimate that $V_0 \approx 10^{-2}$ m s⁻¹. The coefficient A is then calculated as

$$A = \frac{\rho V_0}{s} \sqrt{\frac{\mu}{\rho} \frac{s}{\ln \gamma}} \approx 10^{-3} \frac{s}{\ln \gamma}.$$

If $s=1$ and $\gamma=2$ then

$$A \approx 10^{-3}.$$

This value for A is in agreement with the value expected from rock-friction experiments of A from 10^{-3} to 10^{-2} [9].

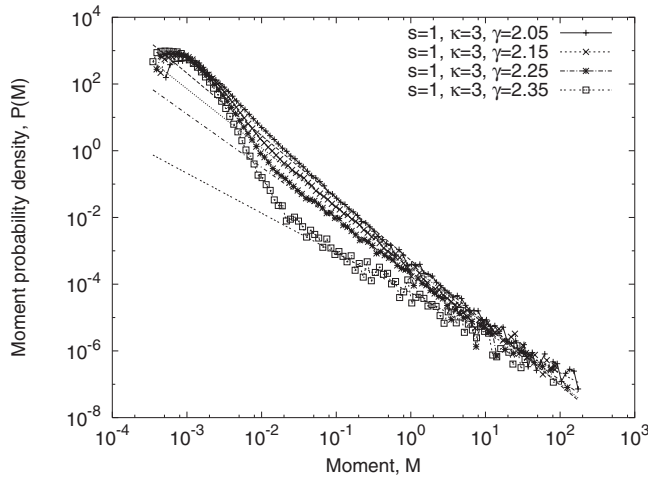


FIG. 8. The moment PDDs for a 100 block system with $s=1$, $\kappa=3$, and increasing γ from the point of power-law behavior toward small scale behavior. Power laws are fitted to the large scale of the PDDs showing a decreasing exponent magnitude with increasing γ .

The frictional parameter A near the transition is then consistent with real earthquake systems.

Figure 8 shows the moment PDDs for a 100 block system in the range $\gamma \in [2.05, 2.35]$. There are two general features of these PDDs. First, large scale moments are power-law distributed having an exponent magnitude that decreases with increasing γ . Second, small scale moments appear to follow a distribution similar to lognormal or exponential distributions. In contrast to the power-law behavior here, Ohmura and Kawamura [9] observed near periodic large scale events dominating the distribution of moments for their investigation of the Dieterich and Ruina state variable friction laws. However, in Ohmura's work the stiffness parameter $l = \frac{k_c}{k_t} = 3$, whereas here $k_c = k_t$. The parameter space where $k_c > k_t$ has been shown to exhibit large scale quasiperiodic delocalized events that are lost when $k_c = k_t$ [17].

The variation in the power-law exponent is of interest because, if the system is critical throughout, a changing power-law exponent suggests the absence of a universality class for the system.

Schorlemmer *et al.* [28] investigated the variation in b values based on earthquake catalogs and found an approximate range for the b value from 0.6 to 1.1. Figure 9 shows the tuning of the power-law exponent of the distribution of moments measured in the model investigated here. In earthquake systems the b value is the exponent associated with the cumulative probability distribution of magnitudes of events [29]. The power-law exponent of the distribution of moments measured here is then $b+1$. The range of exponents through the transition seen in Fig. 9 is from about 1.4–1.9. Here the measured exponent for $\gamma=2.35$ is ignored due to the large uncertainty of the measure. These power-law exponents yield b values from 0.4 to 0.9, similar to those expected for real earthquake faults.

A varying power-law exponent is also seen in the OFC model [10] with a larger range of b values to the range observed in both Fig. 9 and real earthquake systems. The range observed in the OFC model spans b values from less than 0.5

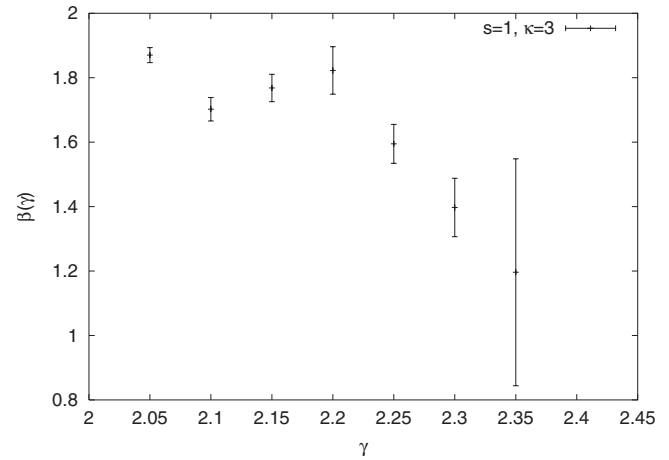


FIG. 9. The power-law exponents associated with the large scales of the moment PDDs.

to approximately 2.5 [10], far beyond the bounds of what is observed in nature. It could be that the large and small scale dynamic phases, particularly the former that is not observed in the OFC model, preclude the b values outside the ranges seen in nature and here in the BK model.

The OFC model does not exhibit any small scale feature such as that observed here. A system with a region, as opposed to a point, in parameter space that exhibits power-law behavior might be considered a bounded SOC system, as indeed the OFC model is. However, this cannot be the case here because of the presence of the small scale feature that must have an associated scale. It must be determined if this small scale feature is a numerical artifact or not. This small scale feature is not a numerical time integration artifact based on experiments that varied the time step. The resulting moment PDDs for different time steps showed no significant differences indicating that the small scale feature is a valid feature of the numerical solution.

In contrast, the small scale feature is dependent on the perturbation used to initiate events as can be seen in Fig. 10. As the perturbation is decreased the small scale feature recedes to smaller and smaller scales while exposing a greater extent of the power law. While the perturbation is a numerical tool in this model, it is postulated that the small scale feature is a reflection of the creep behavior of the small scale phase while the power-law feature represents events in the stick-slip phase, i.e., the two dynamic phases coexist. Creep events in real earthquake systems are small events that attain only small velocities. They also occur at a nearly constant rate on large time scales accounting for the “secular creep on the fault” [30]. Yet creep behavior is also found alongside the power-law distributed behavior usually associated with earthquakes. Indeed, a laboratory experiment of stick-slip behavior has also been seen to exhibit a mixed phase [31]. It may then come as no surprise that a mixed stick-slip/creep phase is observed here.

From the results above, in the order of increasing γ the system exhibits a large scale phase, power-law moment PDD, a mixed phase of power-law distributed large events and creep, and a creep phase. Large scale power laws are observed over a region of parameter space that must occupy

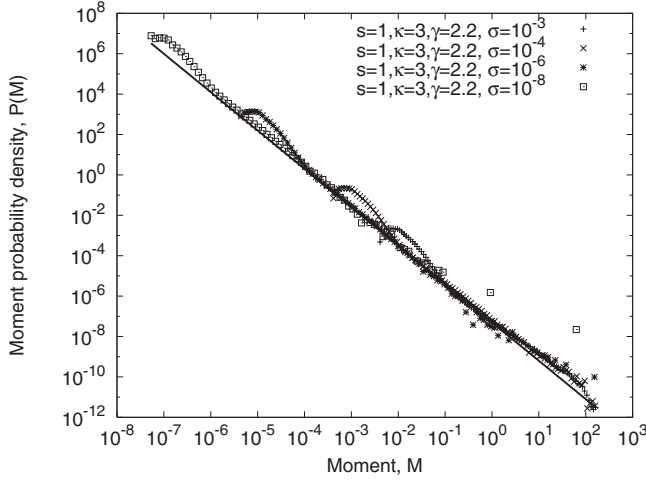


FIG. 10. The effect of different perturbations on the small scale feature. Shown are the PDDs for different perturbations using 10^7 events. The PDDs have been vertically translated to show that the underlying power-law behavior is unmodified.

a finite volume, with exponents varying in a range similar to that of real earthquake behavior and a range that is a subset of those seen in the OFC model.

VI. CONCLUSIONS

The Burridge-Knopoff (BK) model has been investigated with a variant of the Dieterich state variable friction law that more realistically represents rock friction. In this work it has been shown that the Carlson and Langer friction law is equivalent to the Dieterich friction law in the limit that the steady-state coefficient of friction μ_{ss} tends to zero for infinite slip rate, μ_{ss} tends to a finite value for zero slip rate, and the two velocity scales of the Dieterich law become equal. The Dieterich friction law has been modified by ensuring a linear growth of the state variable during quiescence to allow the system to remain well defined at zero slip rate and retain the logarithmic increase in friction with time empirically observed in real rock friction. Applying this friction law to a single-block system, an apparent first-order transition is seen as previously found for the Carlson and Langer law. For a multiblock system, using the Dieterich law operating in a region of parameter space consistent with real rock friction, a continuous transition from large scale event size to small scale event size is observed. Near this transition, event sizes are distributed as a power law with exponents that vary as the transition is approached, suggesting the absence of universality in the system. In addition, this exponent may be tuned leading to b values over an approximate range of 0.4–0.9, which encompasses much of the range of b values observed in nature, observed to be approximately from 0.6 to 1.1 [28].

ACKNOWLEDGMENT

We gratefully acknowledge Enterprise Ireland for funding this research.

APPENDIX: NONDIMENSIONALIZATION OF THE BK MODEL

Nondimensionalization of Eq. (10) is performed using Eq. (A1)

$$x = l_x x^*, \quad (\text{A1a})$$

$$y = l_y y^*, \quad (\text{A1b})$$

$$t = \tau_Q t_Q = \tau_A t_A, \quad (\text{A1c})$$

$$\bar{v}/V_0 = \frac{\tau_A}{\tau_Q}, \quad (\text{A1d})$$

$$\sqrt{\frac{\lambda + 2\mu}{\rho}} = \frac{l_x}{\tau_A}, \quad (\text{A1e})$$

$$\sqrt{\frac{2\mu}{\rho}} = \frac{l_y}{\tau_A}, \quad (\text{A1f})$$

$$V_k/V_0 = v_k, \quad (\text{A1g})$$

$$V_1/V_0 = \gamma, \quad (\text{A1h})$$

$$\vartheta_k/V_0 = \theta_k, \quad (\text{A1i})$$

$$b = \tau_A, \quad (\text{A1j})$$

$$sA/V_0 = \frac{\rho l_y}{\tau_A} \frac{s}{\ln \gamma}, \quad (\text{A1k})$$

$$F_k/V_0 = \frac{1}{\tau_A} f_k, \quad (\text{A1l})$$

$$\Phi^D/V_0 = \frac{\rho l_y}{\tau_A} \phi^D, \quad (\text{A1m})$$

$$\mathcal{T}_k/V_0 = \frac{\rho l_y}{\tau_A} T_k, \quad (\text{A1n})$$

$$k_c = (\Delta x^*)^{-2}, \quad (\text{A1o})$$

$$k_t = (\Delta y^*)^{-2}, \quad (\text{A1p})$$

where t_Q is the time measured during quiescence and t_A that measured during activity, the corresponding scales are τ_Q and τ_A , respectively.

Equations (A1a)–(A1c) are assigning appropriate length and time scales for the system. The other choices for nondimensionalization can be understood by dividing Eqs. (10a)–(10c) by V_0 yielding

$$\frac{d}{dt} \frac{V_k}{V_0} = \frac{F_k}{V_0} - \frac{\Phi^D(V_k, \rho \Delta y F_k)}{V_0 \rho \Delta y}, \quad (\text{A2a})$$

$$\frac{dF_k}{dt V_0} = \frac{\lambda + 2\mu}{\rho\Delta x^2} \left(\frac{V_{k+1}}{V_0} + \frac{V_{k-1}}{V_0} - 2\frac{V_k}{V_0} \right) + \frac{2\mu}{\rho\Delta y^2} \left(\frac{\bar{v}}{V_0} - \frac{V_k}{V_0} \right), \quad (\text{A2b})$$

$$\frac{d\vartheta_k}{dt V_0} = \frac{V_k}{bV_0} \left[1 - \frac{V_0\vartheta_k}{V_0V_1} \right] + \frac{\vartheta_k}{V_k} \frac{dV_k}{dt V_0}. \quad (\text{A2c})$$

This suggests the set of nondimensional variables associated with Eqs. (A1g)–(A1i). In addition, it is noted that F_k is an acceleration and so the fraction $\frac{F_k}{V_0}$ has the dimensions of inverse time. The scale associated with this is the active time scale τ_A , leading to Eq. (A1l).

Using Eqs. (A1g)–(A1i) and (A1l) result in

$$\frac{dv_k}{dt} = \frac{f_k}{\tau_A} - \frac{\Phi^D(V_k, \rho\Delta y F_k)}{V_0\rho\Delta y}, \quad (\text{A3a})$$

$$\frac{1}{\tau_A} \frac{df_k}{dt} = \frac{\lambda + 2\mu}{\rho\Delta x^2} (v_{k+1} + v_{k-1} - 2v_k) + \frac{2\mu}{\rho\Delta y^2} \left(\frac{\bar{v}}{V_0} - v_k \right), \quad (\text{A3b})$$

$$\frac{d\theta_k}{dt} = \frac{v_k}{b} \left[1 - \frac{\theta_k}{\gamma} \right] + \frac{\theta_k}{v_k} \frac{dv_k}{dt}. \quad (\text{A3c})$$

The constants $\frac{\bar{v}}{V_0}$ and b are still in dimensional form but may be associated with time scales.

The first of these, $\frac{\bar{v}}{V_0}$, is a ratio of two velocity scales and is therefore already dimensionless, but how is this related to the scales of the system? Both velocities are in the x direction and as such are associated with the length scale l_x . However, \bar{v} is a very slow velocity associated with the driving and hence quiescent time scale τ_Q . In contrast, V_0 is a velocity associated with the dynamic friction and may be associated with the active time scale τ_A . The ratio of the two velocity scales then results in Eq. (A1d).

The second example b is a parameter associated with the dynamic friction. This parameter has the dimensions of time

and is a natural choice in defining the active time scale τ_A leading to Eq. (A1j).

Equations (A1k), (A1m), and (A1n) are all associated with nondimensionalizing a shear stress. Shear stress has dimensions of force per unit area. For example, the shear stress \mathcal{T} in Eq. (A1n) may be decomposed as

$$\mathcal{T} = \left(\frac{\rho l_x l_y l_z}{l_x l_z} \right) \frac{l_x}{\tau_A^2} \mathcal{T} = \mathcal{T} \frac{\rho l_x l_y}{\tau_A^2},$$

where x and z are the orthogonal axes defining the frictional contact area $l_x l_z$. Equation (A1n) follows from the relation $V_0 \propto \frac{l_x}{\tau_A}$. The same arguments hold for Eqs. (A1k) and (A1m).

Finally, the compressional and transverse wave speeds associated with the bulk medium are $\sqrt{\frac{\lambda+2\mu}{\rho}}$ and $\sqrt{\frac{\mu}{\rho}}$, respectively. These waves have velocity along the x and y directions, respectively, and so the substitutions of Eqs. (A1e) and (A1f) may then be made.

In addition to all these, the substitutions of Eqs. (A1o) and (A1p) are made where the nondimensional discretizations Δx^* and Δy^* are associated with the spring constants of the BK model. Equation (A3) becomes (with simplification)

$$\tau_A \frac{dv_k}{dt} = f_k - k_t^{1/2} \phi^D, \quad (\text{A4a})$$

$$\tau_A \frac{df_k}{dt} = k_c (v_{k+1} + v_{k-1} - 2v_k) + k_t \left(\frac{\tau_A}{\tau_Q} - v_k \right), \quad (\text{A4b})$$

$$\frac{d\theta_k}{dt} = \frac{v_k}{\tau_A} \left[1 - \frac{\theta_k}{\gamma} \right] + \frac{\theta_k}{v_k} \frac{dv_k}{dt}. \quad (\text{A4c})$$

The same substitutions may be made for Eq. (9) leading to Eq. (11). Note that the time t has not as yet been nondimensionalized. There is a choice associated with this step as implied by Eq. (A1c) where two possibilities are given, either $t = \tau_Q t_Q$ or $t = \tau_A t_A$, and each choice results in Eqs. (12) and (14), respectively.

-
- [1] R. Burridge and L. Knopoff, *Bull. Seismol. Soc. Am.* **57**, 341 (1967).
 [2] J. M. Carlson and J. S. Langer, *Phys. Rev. A* **40**, 6470 (1989).
 [3] J. M. Carlson and J. S. Langer, *Phys. Rev. Lett.* **62**, 2632 (1989).
 [4] J. M. Carlson, J. S. Langer, B. E. Shaw, and C. Tang, *Phys. Rev. A* **44**, 884 (1991).
 [5] J. M. Carlson, *Phys. Rev. A* **44**, 6226 (1991).
 [6] J. M. Carlson, *J. Geophys. Res., [Solid Earth Planets]* **96**, 4255 (1991).
 [7] J. M. Carlson, J. S. Langer, and B. E. Shaw, *Rev. Mod. Phys.* **66**, 657 (1994).
 [8] B. E. Shaw and J. R. Rice, *J. Geophys. Res., [Solid Earth]* **105**, 23791 (2000).
 [9] A. Ohmura and H. Kawamura, *Europhys. Lett.* **77**, 69001 (2007).
 [10] Z. Olami, Hans Jacob S. Feder, and K. Christensen, *Phys. Rev. Lett.* **68**, 1244 (1992).
 [11] I. Clancy and D. Corcoran, *Phys. Rev. E* **71**, 046124 (2005).
 [12] P. Bak, *Physica A* **163**, 403 (1990).
 [13] J. Dieterich, *J. Geophys. Res.* **77**, 3690 (1972).
 [14] J. Dieterich, *J. Geophys. Res.* **84**, 2161 (1979).
 [15] A. Ruina, *J. Geophys. Res.* **88**, 10359 (1983).
 [16] J. H. Dieterich, *Tectonophysics* **211**, 115 (1992).
 [17] I. Clancy and D. Corcoran, *Phys. Rev. E* **73**, 046115 (2006).
 [18] M. S. Paterson and T.-f. Wong, *Experimental Rock Deformation—the Brittle Field*, 2nd ed. (Springer, New York, 2005), Chap. Friction and Sliding Phenomena, p. 167.
 [19] This can be seen in a simple transformation of variables. Assuming μ_0 is nonzero leads to an additional term in Eq. (10a): $-\frac{\sigma}{\rho\Delta y}\mu_0$. Performing the transformation $F_k \mapsto F_k + \frac{\sigma}{\rho\Delta y}\mu_0$, the dependence of Eqs. (9) and (10) defining the model reduces to

exactly the same form as if $\mu_0=0$. The original F_k may be recovered by performing the inverse mapping, which is simply adding $\frac{s}{\rho\Delta y}\mu_0$ to F_k .

- [20] C. H. Scholz, *The Mechanics of Earthquakes and Faulting* (Cambridge University Press, New York, 1990).
- [21] J. M. Carlson, E. R. Grannan, and G. H. Swindle, *Phys. Rev. E* **47**, 93 (1993).
- [22] J. M. Carlson, E. R. Grannan, C. Singh, and G. H. Swindle, *Phys. Rev. E* **48**, 688 (1993).
- [23] J. M. Carlson, J. T. Chayes, E. R. Grannan, and G. H. Swindle, *Phys. Rev. Lett.* **65**, 2547 (1990).
- [24] G. L. Vasconcelos, *Phys. Rev. Lett.* **76**, 4865 (1996).
- [25] M. de Sousa Vieira, G. L. Vasconcelos, and S. R. Nagel, *Phys. Rev. E* **47**, R2221 (1993).
- [26] This can be understood by considering t_A (activity) to be measured in seconds (short-time scale) and t_Q (quiescence) to be measured in years (long-time scale). If time in seconds is transformed into time in years and $t = \tau_A t_A = \tau_Q t_Q$ is the (nondimensional) number of years, t_Q , is much smaller than t_A necessitating $\frac{\tau_A}{\tau_Q} \ll 1$. If this separation of time scales is taken to its infinite limit $\frac{\tau_A}{\tau_Q} \rightarrow 0$.
- [27] G. Di Toro, S. Nielsen, and G. Pennacchioni, *Nature (London)* **436**, 1009 (2005).
- [28] D. Schorlemmer, S. Wiemer, and M. Wyss, *Nature (London)* **437**, 539 (2005).
- [29] D. L. Turcotte, *Fractals and Chaos in Geology and Geophysics*, 2nd ed. (Cambridge University Press, Cambridge, London, 1997).
- [30] M. E. Belardinelli, *Phys. Chem. Earth* **21**, 253 (1996).
- [31] A. Johansen, P. Dimon, C. Ellegaard, J. S. Larsen, and H. H. Rugh, *Phys. Rev. E* **48**, 4779 (1993).